International Journal of Heat and Fluid Flow 29 (2008) 1402–1410

Contents lists available at ScienceDirect

International Journal of Heat and Fluid Flow

journal homepage: www.elsevier.com/locate/ijhff

# Drag coefficient in one-dimensional two-group two-fluid model

Yang Liu [a,*], Takashi Hibiki [a], Xiaodong Sun [b], Mamoru Ishii [a], Joseph M. Kelly [c]

[a] School of Nuclear Engineering, Purdue University, 400 Central Drive, West Lafayette, IN 47907-2017, USA
[b] Department of Mechanical Engineering, The Ohio State University, 201 West 19th Avenue, Columbus, OH 43210, USA
[c] US Nuclear Regulatory Commission, Mail Stop: T10K8, Washington, DC 20555, USA

ARTICLE INFO

*Article history:*
Received 13 July 2007
Received in revised form 29 June 2008
Accepted 30 June 2008
Available online 20 August 2008

*Keywords:*
Drag coefficient
Relative velocity
Interfacial area concentration
Interfacial area transport equation
Two-fluid model
Bubbly flow

ABSTRACT

Recently, the concept of the interfacial area transport equation has been proposed to predict the dynamic change of interfacial structure in transient and developing flows. In this approach, bubbles are categorized into two groups (group 1: spherical/distorted bubbles; group 2: cap/slug/churn-turbulent bubbles) due to the considerable difference in their transport characteristics. In this paper, the equations for calculating drag coefficients of both groups under developing flow conditions are derived based on the momentum equations in the one-dimensional two-group two-fluid model. It is found that void fraction of both groups should be taken into account in determining drag coefficient of each group. The shape factor is important for group 2 bubbles even though it can be approximated to be unity for group 1 bubbles. Experimental data of air–water upward bubbly flows in various sizes of pipes are used to examine the existing drag coefficient model of group 1 bubbles. It is shown that the Ishii and Chawla's models for spherical and distorted bubbles can predict the experimental data in the forced convective flow systems satisfactorily, which confirms their applicability to bubbly flow systems.



## 1. Introduction

In solving two-phase flows using the two-fluid model, a key issue is to accurately predict the interfacial transfer terms which link two separate phases in the mass, momentum and energy balance equations. The interfacial area concentration thus becomes very important since those interfacial transfer terms are directly related to it. Traditionally, the interfacial area concentration is modeled based on flow regimes and their transition criteria. However, this approach can not reflect the dynamic nature of the interfacial structure and may induce numerical oscillations in thermal-hydraulic system analysis codes for nuclear reactors. In order to overcome those shortcomings and be consistent with the two-fluid model, the foundation of interfacial area transport equation has been established based on the population balance method (Kocamustafaogullari and Ishii, 1995). It was followed by extensive studies both theoretically and experimentally to formulate the interfacial area transport equation and to model the source and sink terms for a wide range of two-phase flow conditions (Wu et al., 1998; Hibiki and Ishii, 2000a,b; Fu and Ishii, 2002a,b; Kim et al., 2002; Sun et al., 2004a,b).

Various bubbles with different sizes and shapes exist in two-phase flows, which can cause substantial differences in their transport characteristics due to the differences in drag force and bubble interaction mechanisms. A two-group approach has been proposed (Hibiki and Ishii, 2000b; Fu and Ishii, 2002a; Sun et al., 2004b; Ishii and Hibiki, 2005) to account for those differences in the modeling of interfacial area transport. In the two-group interfacial area transport equation, in terms of the bubble size, shape and hence the transport phenomena, bubbles are categorized into two groups: spherical/distorted bubbles as group 1 and cap/slug/churn-turbulent bubbles as group 2. Preliminary strategy of modifying the conventional two-fluid model has been developed to implement the two-group interfacial area transport equation (Sun et al., 2003). In this strategy, interfacial mass transfer, interfacial drag, and interfacial heat transfer are partitioned into two groups, corresponding to the two groups of bubbles. In the modified two-fluid model, the drag coefficient and interfacial heat transfer coefficient for each group need to be specified as constitutive relations. In this paper, a study of the interfacial drag force is presented.

The drag coefficient of a single particle, including gas bubble, liquid droplet and solid particle has been studied extensively (Wallis, 1974; Clift et al., 1978; Khan and Richardson, 1987; Tomiyama et al., 1998). For solid particles in multi-particle systems, considerable work has been done to study the relationship between the particle concentration and relative velocity in the fluidization/sedimentation process (for example, Richardson and Zaki, 1954; Khan and Richardson, 1989). Based on these studies, the drag coefficient for solid particles in multi-particle systems can be obtained accordingly (Khan and Richardson, 1990). In the gas–liquid two-phase

* Corresponding author. Tel.: +1 765 496 3902; fax: +1 765 494 5951.
*E-mail address:* liu130@purdue.edu (Y. Liu).

0142-727X/$ - see front matter © 2008 Elsevier Inc. All rights reserved.
doi:10.1016/j.ijheatfluidflow.2008.06.006

**Nomenclature**

| | |
|---|---|
| $A$ | cross sectional area |
| $a_i$ | interfacial area concentration |
| $B_d$ | volume of a typical bubble |
| $C_0$ | volumetric-flux-distribution parameter |
| $C_D$ | drag coefficient |
| $D$ | pipe diameter |
| $D_C$ | maximum distorted bubble limit |
| $D_{Sm}$ | bubble Sauter mean diameter |
| $g_z$ | gravitational acceleration along vertically downward direction |
| $j$ | superficial velocity |
| $N_{Re}$ | particle Reynolds number |
| $N_{\mu f}$ | viscosity number of liquid phase |
| $p$ | pressure |
| $r_b$ | bubble radius |
| $r_D$ | bubble drag radius |
| $r_{Sm}$ | bubble Sauter mean radius |
| $t$ | time |
| $\upsilon$ | velocity |
| $\upsilon_r^*$ | non-dimensional relative velocity |
| $Z$ | axial distance |

*Greek symbols*

| | |
|---|---|
| $\alpha$ | void fraction |
| $\Delta\rho$ | density difference between phases |
| $\mu$ | dynamic viscosity |
| $\rho$ | density |
| $\sigma$ | surface tension |

*Subscripts*

| | |
|---|---|
| 0 | test section inlet |
| 1 | group 1 bubbles |
| 2 | group 2 bubbles |
| f | liquid |
| g | gas |
| i | interface |
| $k$ | index |
| cal. | calculated value |
| exp. | experimental result |

*Symbols*

| | |
|---|---|
| $\langle\rangle$ | area-averaged quantity |
| $\langle\langle\rangle\rangle$ | void fraction weighted cross-sectional area-averaged quantity |

systems the drag coefficient becomes more complicated since gas bubbles can be deformed due to liquid turbulence, interface interaction and phase change. Similar to solid particles, the studies were mostly focusing on correlating drag coefficient with void fraction (Davidson and Harrison, 1966; Ishii and Chawla, 1979; Garnier et al., 2002; Behzadi et al., 2004). Among them the drag models developed by Ishii and Chawla (1979) by assuming similarity between drag coefficients in single and multiple particle systems seem to be mechanistically based. They were hence proposed to be used as constitutive relations in the two-fluid model (Ishii and Mishima, 1984). In their study, the gas-liquid two-phase flows were categorized into Stokes regime, viscous regime, distorted bubble regime, churn-turbulent flow regime and slug flow regime. The comparison of their theoretical predictions with over 1000 experimental data mostly obtained in stagnant liquid systems showed that satisfactory agreement could be obtained for a wide range of the particle concentration and particle Reynolds number.

However, the partition of bubbles into two groups was not considered in the previous study of drag coefficient. It is apparent that small spherical and distorted bubbles have different drag coefficients from large cap, slug, or churn-turbulent bubbles. Therefore, the models developed previously must be evaluated for each group in the two-group two-fluid model, especially for flow conditions where both groups are present. In addition, most of the data which were used to evaluate drag coefficient were taken for flow conditions with low liquid velocities. The applicability of those models at higher liquid velocities needs to be assessed. Furthermore, the major advantage of implementing the interfacial area transport equation into the two-fluid model is to predict the dynamic change of interfacial structure. Therefore, it is important to evaluate the prediction accuracy of those constitutive models for developing flows, where changes of interfacial area concentration in space and/or time are involved.

In view of the above, the equations to determine the drag coefficients of two groups of bubbles are derived based on the gas momentum equations in the two-group two-fluid model. To be consistent with the present one-dimensional thermal-hydraulic analysis codes, the equations are averaged over the cross sectional area of flow channel to obtain the one-dimensional model. In the first phase of this research, the data taken in bubbly flow regime are used to evaluate the drag coefficient of group 1 bubbles developed by Ishii and Chawla (1979). Due to the lack of experimental data and other difficulties such as determining the bubble shape factor, the study of drag coefficient of group 2 bubbles is currently ongoing and will be reported in the future.

## 2. Drag coefficient in two-group two-fluid model

### 2.1. Evaluation scheme of drag coefficient

Drag coefficient is not a directly measurable parameter. For a single object, one can calculate the drag force based on the force balance equation and hence determine the drag coefficient if other parameters such as fluid density, projected area and relative velocity are known (Ishii and Hibiki, 2005). For multiple particle system, one has to start from the momentum equation in the two-fluid model. Based on certain assumptions, the general evaluation scheme of one-dimensional drag coefficients for two groups of bubbles can be obtained:

$$C_{D1} = \frac{8\langle\alpha_1\rangle(1-\langle\alpha_1\rangle-\langle\alpha_2\rangle)\Delta\rho g_z}{\rho_f\langle a_{i1}\rangle\langle v_{r1}\rangle^2}, \tag{1}$$

and

$$C_{D2} = \frac{8\langle\alpha_2\rangle(1-\langle\alpha_1\rangle-\langle\alpha_2\rangle)\Delta\rho g_z}{\rho_f\langle a_{i2}\rangle\langle v_{r2}\rangle^2}\left(\frac{r_D}{r_{sm}}\right)_2. \tag{2}$$

where $\langle\,\rangle$ represents area averaging operator. $C_{Dk}$, $\alpha_k$, $\Delta\rho$, $g_z$, $a_{ik}$ and $v_{rk}$ (here subscript $k = 1, 2$ stands for group 1 or group 2 bubbles) are the drag coefficient, void fraction, density difference, gravitational acceleration along vertically downward direction, interfacial area

concentration and relative velocity between group $k$ bubbles and liquid, respectively. $r_{Smk}$ and $r_{Dk}$ are the Sauter mean radius and the drag radius which are defined as follows:

$$r_{Sm} = \frac{3B_d}{A_i}, \tag{3}$$

and

$$r_D = \frac{3B_d}{4A_d}, \tag{4}$$

where $B_d$, $A_i$ and $A_d$ are the volume, surface area and projected area of a typical bubble, respectively. The boundary between two groups of bubbles, $D_c$, is given by the volume-equivalent diameter for the maximum distorted bubble limit:

$$D_c = 4\sqrt{\frac{\sigma}{g_z \Delta\rho}}, \tag{5}$$

where $\sigma$ is the surface tension.

It can be seen from Eqs. (1) and (2) that measured void fraction, interfacial area concentration and relative velocity for both groups are required to experimentally determine the drag coefficient. Shape factor term $r_D/r_{sm}$ can be assumed to be unity for group 1 bubbles considering the shape is very close to sphere. However it must be taken into account for group 2 bubbles. It is also interesting to see that $C_{D1}$ depends on void fraction of both group 1 and group 2 bubbles. The appearance of group 2 bubbles actually modifies the pressure field and reduces the buoyancy force acting on group 1 bubbles. Similar effect can be also seen in the equation for group 2 bubbles. Therefore, extra care must be taken in determining the drag coefficient from experimental data when bubbles are partitioned into two groups.

The void fraction term in Eq. (1) is represented by total void fraction, if no partition was considered for the gas phase. In this case, Eq. (1) is also consistent with the method which Ishii and Chawla (1979) used to determine drag coefficient from measured parameters. Eq. (1) is further reduced to the force balance equation on a single bubble if void fraction of group 1 bubbles becomes zero. It must be pointed out that Eqs. (1) and (2) are merely the simplified form of momentum equations in the two-group two-fluid model. It is an Eulerian approach to determine the drag coefficient that bubbles actually experience in two-phase flows. However, drag coefficients must be given as constitutive models in solving the field equations of the two-fluid model. In developing such constitutive models, one has to start from the Lagrangian approach, namely, force balance on a single bubble, since it does not depend on specific two-phase flows. The above result also shows the consistency of those two approaches.

The ratio of the drag radius to the Sauter mean radius, or the shape factor for group 2 bubbles should be determined to calculate drag coefficient of group 2 bubbles using Eq. (2). A 50° wake angle can be assumed for ideal cap bubbles (Clift et al., 1978), and the shape factor is determined as a constant accordingly. However, in the real two-phase flow the above bubble profile may not be applicable anymore. In slug and churn-turbulent flows, the shape factor for the Taylor bubbles and churn-turbulent bubbles strongly depend on the geometry of the specific flow channels. Considering the availability of experimental data, current study will focus on the drag coefficient of group 1 bubbles only.

### 2.2. Ishii and Chawla's drag coefficients model

Within the scope of group 1 bubbles, Ishii and Chawla (1979) categorized the gas-liquid bubbly flow into three flow regimes, i.e. Stokes regime, viscous regime and distorted particle regime. The present study will only consider the last two flow regimes since Stokes regime applies for very low particle Reynolds number ($N_{Re} < 1$), which is not the cases of the available data.

A constitutive equation of the drag coefficient for viscous regime is given by (Ishii and Chawla, 1979):

$$C_D = \frac{24\left(1 + 0.1N_{Re}^{0.75}\right)}{N_{Re}}, \tag{6}$$

where the particle Reynolds number is defined as:

$$N_{Re} \equiv \frac{2\rho_f |\langle v_r \rangle| \langle r_b \rangle}{\mu_m}. \tag{7}$$

The mixture viscosity for bubbly flow, $\mu_m$, is given by:

$$\frac{\mu_m}{\mu_f} = (1 - \langle\alpha\rangle)^{-1}, \tag{8}$$

where $\mu_f$ is the liquid viscosity. The spherical bubble limit, $D_{max}$, beyond which bubbles become distorted, is given by Ishii and Zuber (1979):

$$D_{max} = 4\sqrt{\frac{2\sigma}{g_z \Delta\rho}} N_{\mu_f}^{1/3}, \tag{9}$$

where the viscosity number of liquid phase is defined as:

$$N_{\mu_f} \equiv \frac{\mu_f}{\left(\rho_f \sigma \sqrt{\frac{\sigma}{g\Delta\rho}}\right)^{1/2}}. \tag{10}$$

A constitutive equation of drag coefficient for distorted-particle regime is given by Ishii and Chawla (1979):

$$C_D = \frac{4}{3}\langle r_b \rangle \sqrt{\frac{\Delta\rho g_z}{\sigma}} \left[\frac{1 + 17.67\{f(\langle\alpha\rangle)\}^{6/7}}{18.67 f(\langle\alpha\rangle)}\right]^2 \simeq \frac{4}{3}\langle r_b \rangle \sqrt{\frac{\Delta\rho g_z}{\sigma}} \frac{1}{(1 - \langle\alpha\rangle)^{0.5}}, \tag{11}$$

where $f(\langle\alpha\rangle) = (1 - \langle\alpha\rangle)^{3/2}$ for bubbly flow.

## 3. Databases used for evaluation of drag coefficient and relative velocity

During the previous study of interfacial area transport of bubbly flows, more forced convective bubbly flow data (Hibiki and Ishii, 1999; Hibiki et al., 2001) are readily available for evaluation of the drag coefficient of group 1 bubbles based on the equations derived above. Comparing with the data that Ishii and Chawla (1979) originally used, the new data were taken at much higher liquid velocities. Most importantly, those data were taken while interfacial structures were still developing, namely, the interfacial area changes along the flow direction due to bubble expansion and interactions. Therefore, the new data can justify the applicability of the drag models when the interfacial area transport equation and the two-fluid model are coupled.

The available experimental data include adiabatic air–water bubbly upward flows in vertical pipes with inner diameters, $D$, of 25.4 and 50.8 mm (Hibiki and Ishii, 1999; Hibiki et al., 2001). Local measurements of void fraction, interfacial area concentration and gas velocity were performed by using the double sensor conductivity probe. Local measurement of liquid velocity was conducted by using hot film anemometry. Cross-calibration results showed that the difference between the area-averaged void fraction, interfacial area concentration, superficial gas velocity and superficial liquid velocity obtained from local measurements and those by gamma densitometer, the photographic method, rotameter and magnetic flow meter were within ±5.74%, ±6.95%, ±12.4% and ±5.19%, respectively. The detailed discussions of local flow parameters are found in the previous papers (Hibiki and Ishii, 1999; Hibiki et al., 2001).

**Table 1**
Experimental conditions of data taken by Hibiki and Ishii (1999) and Hibiki et al. (2001)

| Investigators | $D$ (mm) | Symbols | ● | ▲ | ■ | ▼ | ♦ | * |
|---|---|---|---|---|---|---|---|---|
| | | $\langle j_f \rangle$ (m/s) | $\langle j_{g,0} \rangle$ (m/s) | $\langle j_{g,0} \rangle$ (m/s) | $\langle j_{g,0} \rangle$ (m/s) | $\langle j_{g,0} \rangle$ (m/s) | $\langle j_{g,0} \rangle$ (m/s) | $\langle j_{g,0} \rangle$ (m/s) |
| Hibiki and Ishii (1999) | 25.4 | 0.262 | 0.0549 | 0.0610 | 0.0780 | 0.0990 | 0.117 | N/A |
| | | 0.872 | 0.0414 | 0.0813 | 0.143 | 0.210 | 0.305 | N/A |
| | | 1.75 | 0.0461 | 0.116 | 0.257 | 0.399 | 0.575 | N/A |
| | | 2.62 | 0.0804 | 0.193 | 0.401 | 0.581 | 0.764 | N/A |
| | | 3.49 | 0.0509 | 0.201 | 0.516 | 0.702 | 0.931 | N/A |
| Hibiki et al. (2001) | 50.8 | 0.491 | 0.0275 | 0.0556 | 0.129 | 0.190 | N/A | N/A |
| | | 0.986 | 0.0473 | 0.113 | 0.242 | 0.321 | N/A | N/A |
| | | 2.01 | 0.103 | 0.226 | 0.471 | 0.624 | N/A | N/A |
| | | 5.00 | 0.245 | 0.518 | 1.11 | 1.79 | 2.87 | 3.90 |

N/A: not available.

It must be mentioned that the relative velocities measured at relatively high liquid velocities contain significant measurement error. This can be explained by a simple sensitivity analysis of the propagation of measurement error in determining the relative velocity. For this purpose, the relative velocity can be approximated by the terminal velocity of a single distorted bubble rising in the stagnant water, which is around 0.231 m/s at atmospheric pressure and 20 °C. Since the relative velocity is simply the difference between the gas and liquid velocities, it can be shown that a 5% error in the measurements of gas and liquid velocities results in ±19.2%, ±34.3%, ±64.9%, and ±156.6% errors in relative velocity measurement with the superficial liquid velocities of 0.5 m/s, 1.0 m/s, 2.0 m/s and 5.0 m/s, respectively. In view of this, considerable errors in the relative velocity measurement are expected for the data taken at $\langle j_f \rangle = 5.00$ m/s in the 50.8 mm pipe and $\langle j_f \rangle = 3.49$ m/s in the 25.4 mm pipe.

The measurements were performed at three axial locations of $z/D = 12.0$, 65.0 and 125 for the 25.4 mm pipe, and $z/D = 6.00$, 30.3 and 53.5 for the 50.8 mm pipe. Local data of 15 radial locations ranging from $r/R = 0$ to 0.95 were taken for both test sections.

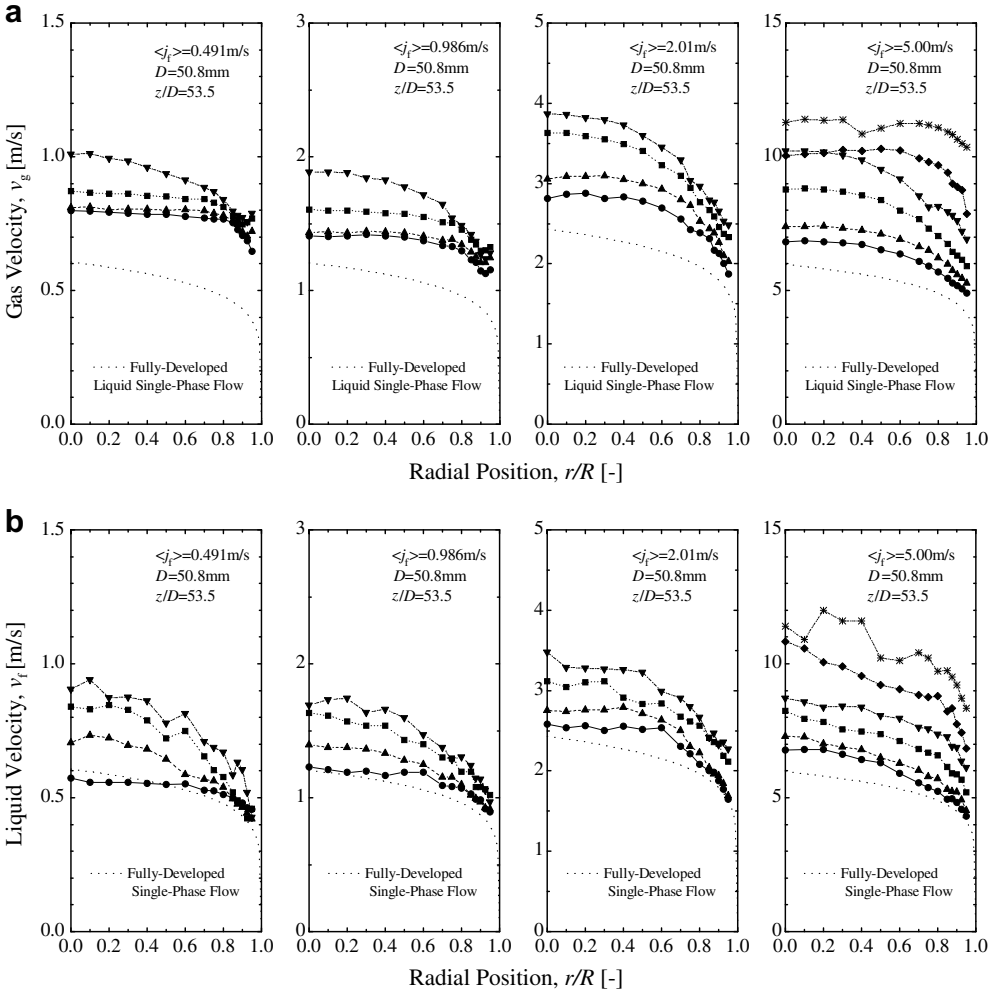


**Fig. 1.** Typical local experimental result obtained in 50.8 mm pipe (Hibiki et al., 2001). (a) Local gas velocity profile and (b) local liquid velocity profile.

The superficial liquid velocity, $\langle j_f \rangle$, ranged from 0.262 m/s to 3.49 m/s for the 25.4 mm pipe and from 0.491 m/s to 5.00 m/s for the 50.8 mm pipe. The inlet superficial gas velocity, $\langle j_{g,0} \rangle$, ranged from 0.0414 m/s to 0.931 m/s for the 25.4 mm pipe and from 0.0275 m/s to 3.90 m/s for the 50.8 mm pipe. The covered void fraction range was from 1.83% to 44.2%. Thus, these data include nearly complete gas and liquid velocity information over wide bubbly flow range including finely-dispersed bubbly flow. The detailed test conditions are given in Table 1. Fig. 1a and b show some typical gas and liquid velocity profiles. In the figure, $r$ and $R$ indicate the radial coordinate measured from the pipe center and pipe radius, respectively, and thus $r/R = 0$ and $r/R = 1$ represent the pipe center and wall, respectively, and the corresponding flow condition of each symbol is found in Table 1. The dotted line in each figure shows the fully developed turbulent velocity profile of single liquid phase flow given by Hibiki et al (1998).

Four other datasets available in the literature (Liu, 1989; Serizawa et al., 1991; Kalkach-Navarro, 1992; Grossetete, 1995) are also considered in evaluating the drag coefficient of group 1 bubbles as listed in Table 2. In those datasets, both liquid velocity and gas velocity were measured for quasi-steady vertical air–water two-phase flows in round pipes. Therefore, the aforementioned assumptions and equations for calculating drag coefficients can be utilized without any modification. Only bubbly flow conditions were considered for the present evaluation of group 1 bubbles.

## 4. Results and discussion

### 4.1. Evaluation of drag coefficient model in viscous regime

The spherical bubble limit is the upper limit for the viscous regime and based on Eq. (5), it is estimated to be 2 mm for a single bubble rising in the stagnant water at atmospheric pressure and 20 °C temperature. Thus, the flow with the bubble size smaller or larger than 2 mm is categorized as viscous or distorted-particle regime, respectively. If the data taken at the highest liquid velocities are not considered due to the significant error discussed above, all other data fall into distorted-particle regime. However, some datasets are very close to the boundary between viscous and distorted-particle regimes. These data will give us some insight on the validity of the drag model in viscous regime, Eq. (6). Fig. 2 shows the comparison of Eq. (6) with experimentally determined drag coefficients with Sauter mean diameter slightly higher than 2 mm. In the figure, the solid line indicates the drag coefficient calculated by Ishii and Chawla's model, Eq. (6). It can be seen that the data obtained in forced convective flow follow the model prediction fairly well. An excellent agreement was also reported when Ishii and Chawla (1979) originally compared Eq. (6) with various experimental data mostly taken in stagnant liquid systems, which provided very accurate drag coefficient data. Combining these experimental results may lead to a conclusion that Eq. (6) can be applied to forced convective bubbly flows or one-group interfacial area transport equation.

### 4.2. Evaluation of drag coefficient model in distorted-particle regime

As can be seen from Eq. (11), the drag coefficient in distorted-particle regime depends on the bubble radius and void fraction rather than solely on the particle Reynolds number. Combining Eqs. (1) and (11) yields the relative velocity in distorted-particle regime as:

$$\langle v_r \rangle = \sqrt{2}\left(\frac{\Delta\rho g\sigma}{\rho_f^2}\right)^{0.25}(1-\langle\alpha\rangle)^{0.75}. \tag{12}$$

The drag coefficient is not a directly measurable parameter and has to be calculated based on the equations derived previously. It actually measures the degree to which two phases are coupled in terms of velocity if other parameters such as physical properties and particle shape are known. In view of this, a non-dimensional relative velocity, $\langle v_r^* \rangle$ is introduced as:

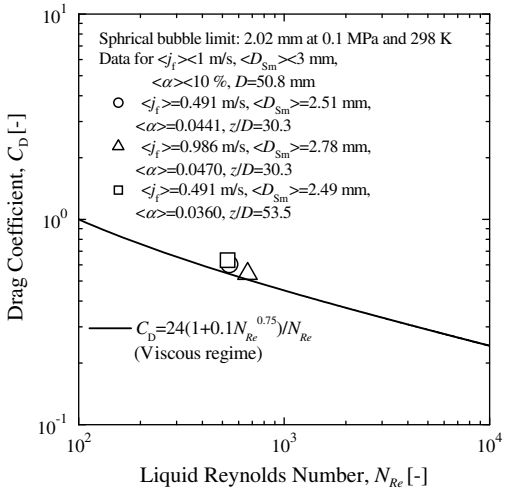


**Fig. 2.** Validation of Ishii-Chawla's drag coefficient model in viscous regime.

**Table 2**
All datasets used in evaluation of the drag coefficient of group 1 bubbles

| Investigators | Geometry and size (mm) | $z/D$ | Pressure (MPa) | Superficial gas velocity (m/s) | Superficial liquid velocity (m/s) | Bubble Sauter mean diameter (mm) | Void fraction | Number of data |
|---|---|---|---|---|---|---|---|---|
| Hibiki and Ishii (1999) | 25.4 ID pipe | 12 | 0.10 | 0.0473–1.12 | 0.262–3.49 | 1.72–3.99 | 0.0155–0.2644 | 25 |
| | | 65 | | 0.0257–1.03 | 0.262–3.49 | 2.19–4.10 | 0.0183–0.2334 | 25 |
| | | 125 | | 0.0562–1.27 | 0.262–3.49 | 2.05–3.99 | 0.0138–0.2825 | 25 |
| Hibiki et al. (2001) | 50.8 ID pipe | 6 | 0.10 | 0.0257–4.45 | 0.491–5.00 | 1.40–3.31 | 0.0360–0.4082 | 18 |
| | | 30.3 | | 0.0328–4.39 | 0.491–5.00 | 1.78–3.52 | 0.0441–0.4059 | 18 |
| | | 53.5 | | 0.0257–4.88 | 0.491–5.00 | 1.77–3.86 | 0.0360–0.4430 | 18 |
| Liu (1989) | 38.1 ID pipe | 30 | 0.10 | 0.0197–0.353 | 0.376–1.39 | 2.12–4.26 | 0.0135–0.4186 | 42 |
| Serizawa et al. (1991) | 60.0 ID pipe | 36 | 0.10 | 0.0941–0.416 | 0.442–1.03 | 3.03–7.75 | 0.0361–0.2523 | 12 |
| Kalkach-Navarro (1992) | 38.1 ID pipe | 50 | 0.10 | 0.0655–0.343 | 0.300–1.25 | 3.35–5.46 | 0.0616–0.2137 | 17 |
| Grossetete (1995) | 38.1 ID pipe | 8 | 0.10 | 0.0577–0.116 | 0.877–1.75 | 2.16–2.70 | 0.0090–0.0471 | 3 |
| | | 55 | | 0.0662–0.133 | 0.877–1.75 | 2.82–3.11 | 0.0535–0.0857 | 3 |
| | | 155 | | 0.0895–0.181 | 0.877–1.75 | 3.37–3.74 | 0.0437–0.0901 | 3 |

$$\langle v_r \rangle \equiv \frac{\langle v_r \rangle}{\langle\langle v_g \rangle\rangle}. \tag{13}$$

It directly reflects the contribution to the total gas velocity which is due to the relative velocity between two phases. For air–water upward flows, $\langle v_r \rangle$ is between 0 and 1 considering that the gas velocity is higher than liquid velocity. The closer this value is to zero, the stronger two phases are coupled in terms of velocity, namely two phases have the same velocity if $\langle v_r \rangle$ is zero. $\langle v_r \rangle = 1$ indicates a stagnant liquid condition. Using this parameter to study the drag coefficient can avoid possible misleading conclusion caused by the large measurement error of relative velocity as discussed above. This is because the non-dimensional relative velocity approaches zero when the liquid velocity is very high. In this case the contribution of relative velocity to the total gas velocity is small such that the results may not be significantly affected by the measurement error.

In Fig. 3, the non-dimensional relative velocities at three different axial locations for the 25.4 mm and 50.8 mm pipes are plotted against the area-averaged void fraction. The open and solid symbols indicate the experimentally determined and calculated non-dimensional relative velocity, respectively. For the 25.4 mm pipe, Fig. 3a–c shows reasonable agreement for all the liquid flow rates. The average value of absolute differences between experimental data and calculated values is 0.043 for all three axial locations. The maximum discrepancy occurs at low liquid velocities (i.e. $\langle j_f \rangle = 0.262$ m/s and $\langle j_f \rangle = 0.872$ m/s) where relative velocity composes as high as 40% of the total gas velocity. At higher liquid velocities, the prediction error of $\langle v_r \rangle$ becomes very small due to stronger coupling between two phases. Both experimental data and calculated values show the same general trend that $\langle v_r \rangle$ decreases with increasing void fraction for a given liquid flow rate. This is due to two reasons: increasing gas velocity and decreasing relative velocity. The former can be explained with help of the drift-flux model (Zuber and Findlay (1965)) as

$$\langle\langle v_g \rangle\rangle = C_0(\langle j_g \rangle + \langle j_f \rangle) + \langle\langle v_{gj} \rangle\rangle, \tag{14}$$

where $C_0$, $j_g$, $j_f$, and $v_{gj}$ are the distribution parameter, superficial gas velocity, superficial liquid velocity and drift velocity, respectively. In the tested flow conditions, the first term in the right hand side is dominant over the second term and the distribution parameter increases with the void fraction (Hibiki and Ishii, 2002). Thus, increased void fraction, namely increased superficial gas velocity for a given flow rate increases the gas velocity. The latter can be seen from Eq. (12). The decreased relative velocity with increased void fraction is a result of increasing drag coefficient when void fraction increases as shown in Eq. (11). Physical explanation of this phenomenon has already been provided by Ishii and Chawla (1979). A particle sees increased drag due to other particles because of the strong contribution of the turbulent eddies in the wake region. In another sense, the existence of multiple particles enhances the coupling between gas bubbles and surrounding liquid.

For the 50.8 mm pipe, Fig. 3d–f shows excellent agreement for all the liquid flow rates except $\langle j_f \rangle = 5.00$ m/s. The average values of absolute differences are 0.068 and 0.022 for $\langle j_f \rangle = 5.00$ m/s and other flow rates, respectively. The void fraction effect has also been correctly predicted by the model except the highest flow rate which may be due to measurement error in relative velocity as mentioned previously.

Fig. 4a and b shows the comparison results for data taken by Liu (1989) in a 30.8 mm pipe. The mean value of absolute differences of all 42 flow conditions is 0.043. Shown in Fig. 4c and d are the

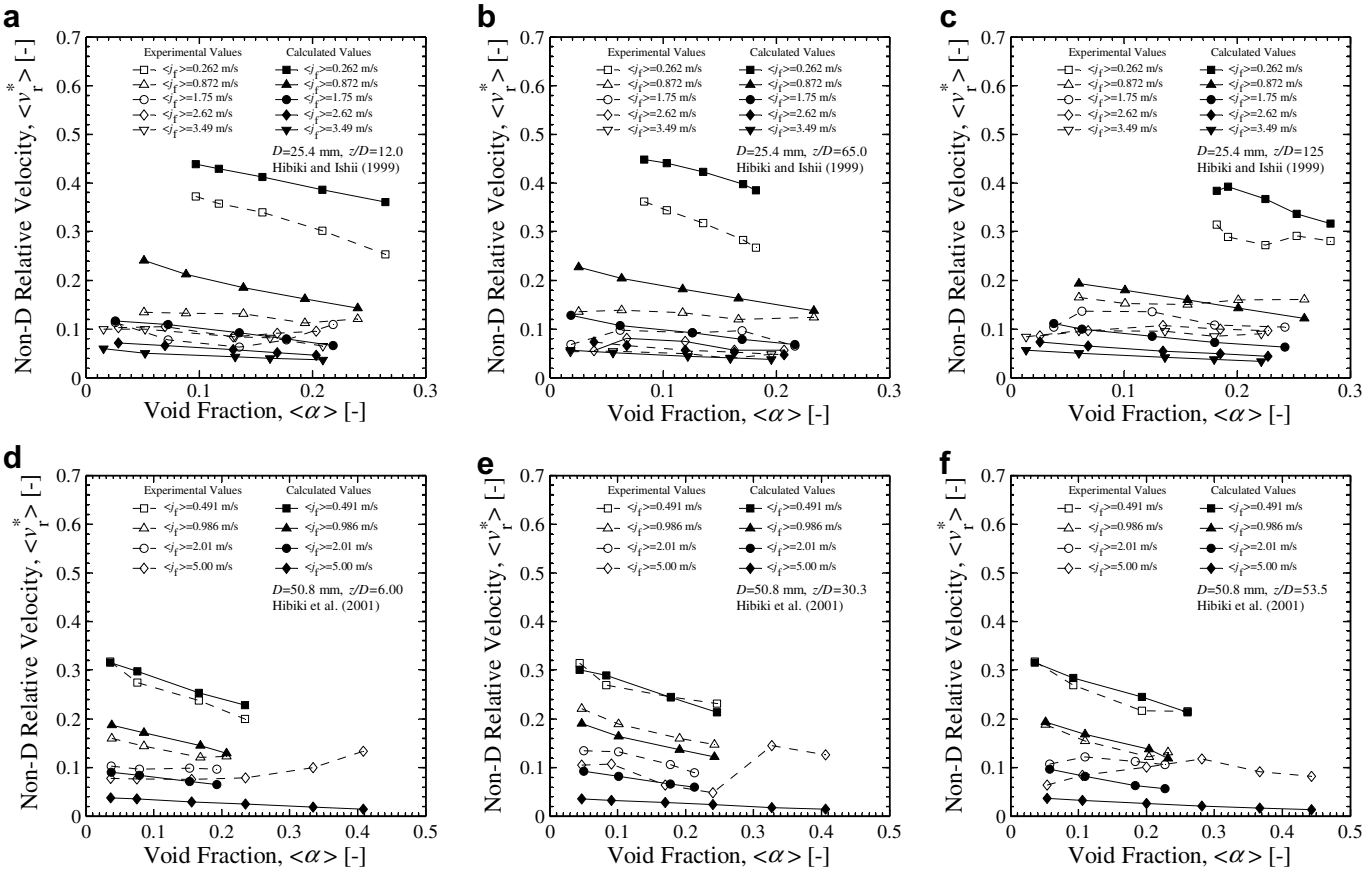


**Fig. 3.** Validation of Ishii-Chawla's drag coefficient model in distorted particle regime using data from Hibiki and Ishii (1999) and Hibiki et al. (2001).

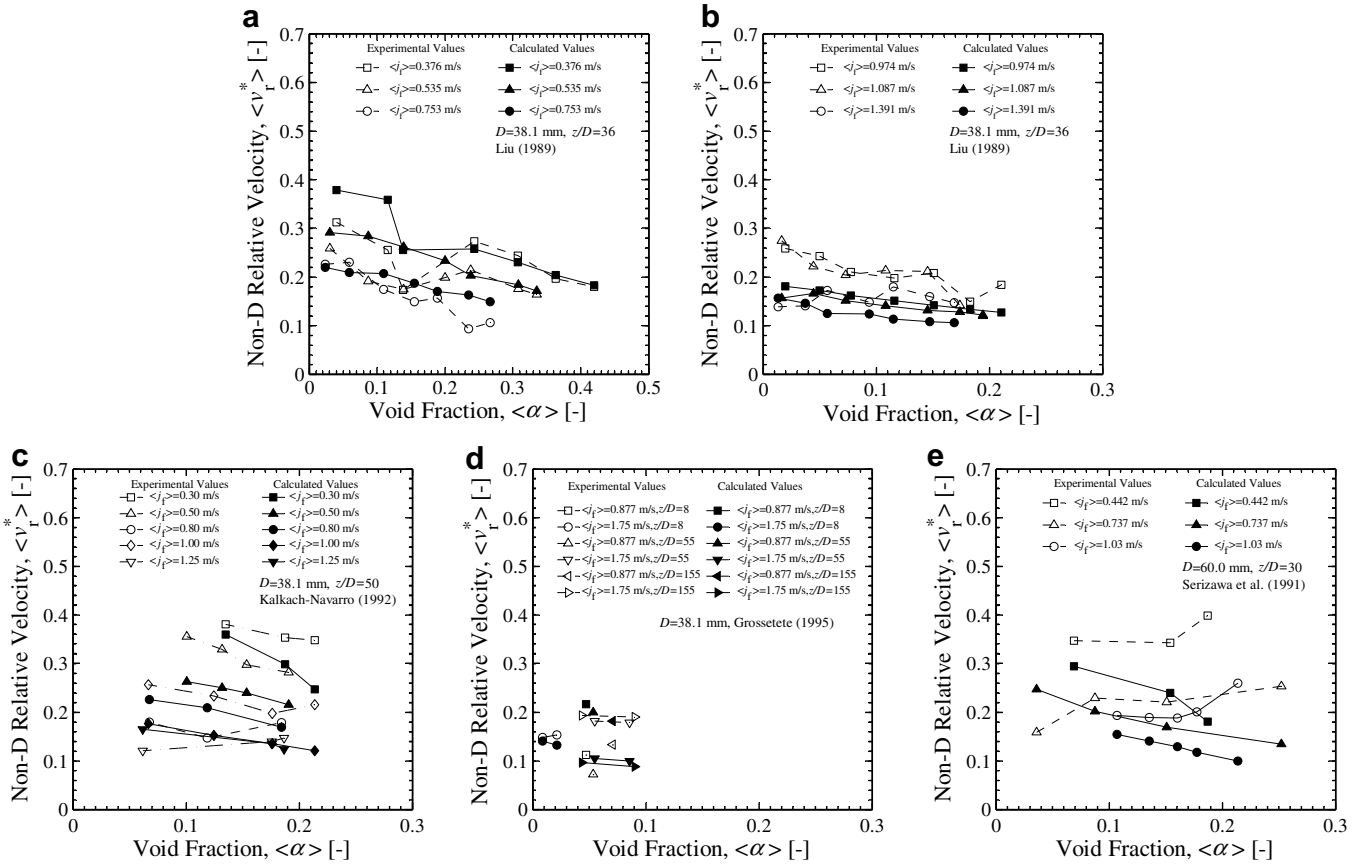


**Fig. 4.** Validation of Ishii-Chawla's drag coefficient model in distorted particle regime using data from other literatures (Liu, 1989; Serizawa et al., 1991; Kalkach-Navarro, 1992; Grossetete, 1995).

comparison results for data taken in pipes with the same inner diameter by Kalkach-Navarro (1992) and Grossetete (1995), respectively. The corresponding mean values of absolute differences are 0.058 and 0.074, respectively. As can be seen in the figure, reasonable agreement can be obtained for these data in terms of both prediction accuracy and general trend. The decreasing trend of $\langle v_r \rangle$ with void fraction is not so obvious in Fig. 4d if comparing with others. It should be noticed that the void fraction range of these data is within 10%. From Eq. (11), the drag coefficient will increase dramatically at higher void fraction. Therefore, the void fraction effect is more apparently shown in Fig. 4a where void fraction is as high as 40%.

The result for data taken by Serizawa et al. (1991) in a pipe with the inner diameter of 60 mm is shown in Fig. 4e. The experimentally determined $\langle v_r \rangle$ shows an increasing trend with increasing void fraction. This is not seen in other data and the model apparently underestimates most of the data. Two possible reasons may account for this result. First, the Sauter mean diameters in Serizawa's data are among the highest (as high as 7.75 mm) and very close to the lower limit of group 2 bubbles ($\sim$10 mm). Thus certain amount of group 2 bubbles might exist in the flow. This results in higher measured relative velocity than that for pure group 1 bubble system since cap and slug bubbles rise faster than distorted bubbles. Secondly, in Serizawa's experiment measurement error was not clearly stated and the results shown in Fig. 4e may be due to some measurement error.

From the above experimental results, it can be seen that the model can predict the velocity coupling between two phases with reasonable accuracy for a wide range of bubbly two-phase flows. It is also noted that most of the data that Ishii and Chawla used to evaluate their drag models were taken from sedimentation, fluidization or batch process (Ishii and Chawla, 1979), where the relative velocity was much more accurately measured since it is essentially the velocity of the moving phase. With those data they obtained very good agreement between the model and experimentally obtained drag coefficient. The present paper is looking at the drag coefficient from the Eulerian point of view which starts from the momentum equation in the two-fluid model. Some data used here were taken for bubbly flows with developing interfacial structure. In this regard, it may be concluded that Ishii and Chawla's drag model can be applied to forced convective bubbly flows or one-group interfacial area transport equation. The effect of group 2 void fraction on the group 1 drag coefficient should be validated to verify the applicability of Eq. (1) and Ishii and Chawla's drag model to two-group two-fluid model in various flow regimes in the future.

It should be mentioned here that the non-dimensional relative velocity shows slightly higher discrepancies for certain data used here. This is partially caused by the error in determining relative velocity from phasic velocities as discussed earlier. However, the measurement error of gas velocity can be usually quantified by cross-calibration method and it is determined to be around ±10%. The comparison of gas velocity is briefly discussed in the Appendix. The results turned out that gas velocity prediction using Ishii and Chawla's drag model is within measurement error range for almost all data that were used here. Considering it is the gas velocity that is solved as one of the unknowns in the two-fluid model, this result confirms the applicability of the model to a wide range of bubbly two-phase flows. However, in a strict sense, this conclusion should be applied to the tested flow conditions such as $25.4\ \text{mm} \leqslant D \leqslant 60.0\ \text{mm}$, $0.0197\ \text{m/s} \leqslant \langle j_g \rangle \leqslant 4.88\ \text{m/s}$, $0.262\ \text{m/s} \leqslant \langle j_g \rangle \leqslant 5.00\ \text{m/s}$ and $6 \leqslant z/D \leqslant 155$. Hibiki and Ishii (2003) developed the drift-flux

model in vertical large diameter pipes. They indicated that the one-dimensional relative velocity at low liquid flow rate might be affected by secondary flow. Thus the applicability of Ishii and Chawla's drag model to a large diameter pipe flow should be examined in the future.

## 5. Summary

In relation to the development of one-dimensional two-group two-fluid model, the approach using two-group drag coefficients in two-group gas momentum equations is studied. Important conclusions are summarized as follows:

(1) Based on the momentum equations in the one-dimensional two-group two-fluid model, a general evaluation scheme is derived to determine the drag coefficients of two groups of bubbles from experimentally measurable parameters. It is found that void fractions of both group 1 and group 2 bubbles should be taken into account to compute the drag coefficient of each group. This is because the existence of the other group modifies the pressure field and hence the buoyancy force acting on bubbles. The derived equation for group 1 bubbles becomes force balance equation for a single bubble when void fraction reduces to zero, which shows the consistency of the Eulerian two-fluid model and Lagrangian approach. The shape factor can not be neglected while evaluating drag coefficient of group 2 bubbles. However, it may be assumed to be unity for group 1 bubbles.

(2) Experimental data of developed and quasi fully-developed air–water upward bubbly flows taken under various pipe size and flow conditions were used to evaluate the existing drag coefficient model for group 1 bubbles. The results indicate that Ishii and Chawla's model can predict the experimental data satisfactorily. A non-dimensional relative velocity is defined to represent the degree to which two phases are coupled. Comparison of this parameter between model prediction and experimental data shows reasonable agreement. It is thus concluded that Ishii and Chawla's model can be applied to forced convective bubbly flows or one-group interfacial area transport equation. The effect of group 2 void fraction on the group 1 drag coefficient should be validated to verify the applicability of Eq. (1) and Ishii and Chawla's drag model to two-group two-fluid model in various flow regimes in the future. Also the applicability of Ishii and Chawla's drag model to a large diameter pipe flow should be examined.

(3) The current study only focuses on group 1 bubbles and experimental data are only available for bubbly flows. However, group 2 bubbles could dominate two-phase flow dynamics when two groups of bubbles coexist (for example, in slug or churn-turbulent flows). In this case the drag coefficient of group 2 bubbles is expected to be more important and it can be determined by the equation derived in this paper, i.e. Eq. (2). The detailed discussion will be covered in the future paper.

## Acknowledgements

The work was performed under the auspices of US Nuclear Regulatory Commission (NRC). The authors would like to express their sincere appreciation for the support.

## Appendix

Ishii and Mishima (1984) proposed an estimation of the area-averaged relative velocity by considering the distribution effect:

$$\langle v_r \rangle \simeq \frac{1 - C_0\langle\alpha\rangle}{1 - \langle\alpha\rangle}\langle\langle v_g\rangle\rangle - C_0\langle\langle v_f\rangle\rangle. \tag{A-1}$$

Combining Eqs. (A-1) and (12), one can estimate the gas velocity based on following equation:

$$\langle\langle v_g\rangle\rangle \simeq \frac{1 - \langle\alpha\rangle}{1 - C_0\langle\alpha\rangle}\left[\sqrt{2}\left(\frac{\Delta\rho g\sigma}{\rho_f^2}\right)^{0.25}(1 - \langle\alpha\rangle)^{0.75} + C_0\frac{\langle j_f\rangle}{1 - \langle\alpha\rangle}\right], \tag{A-2}$$

where $C_0$ is the distribution parameter defined by:

$$C_0 = \frac{\langle\alpha j\rangle}{\langle\alpha\rangle\langle j\rangle}. \tag{A-3}$$

$C_0$ can be obtained experimentally since local void fraction and phasic velocities have been measured in the datasets used here. In case that no local measurement is available, $C_0$ can be also calculated by the well established correlations (for example, Hibiki and Ishii, 2002).

Fig. A1a and b compares the gas velocity estimated by Eq. (A-2) with the experimental data taken by Hibiki et al. and other researchers, respectively. Very good agreement can be seen in both figures where most of the predictions fall into ±10% measurement error range.

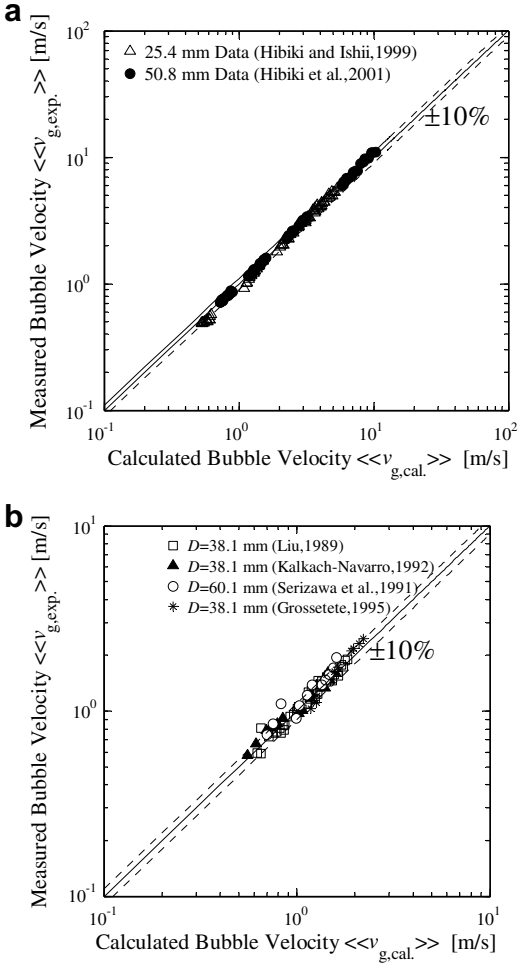


**Fig. A1.** Comparison of predicted gas velocity with experimental data. (a) Data from Hibiki and Ishii (1999) and Hibiki et al. (2001) and (b) data from other literatures (Liu, 1989; Serizawa et al., 1991; Kalkach-Navarro, 1992; Grossetete, 1995).

## References


Behzadi, A., Issa, R.I., Rusche, H., 2004. Modelling of dispersed bubble and droplet flow at high phase fractions. Chemical Engineering Science 59 (4), 759–770.

Clift, R., Grace, J.R., Weber, M.E., 1978. Bubbles, Drops, and Particles. Academic Press, New York.

Davidson, J.F., Harrison, D., 1966. The behaviour of a continuously bubbling fluidised bed. Chemical Engineering Science 21 (9), 731–738.

Fu, X.Y., Ishii, M., 2002a. Two-group interfacial area transport in vertical air–water flow – i. Mechanistic model. Nuclear Engineering and Design 219 (2), 143–168.

Fu, X.Y., Ishii, M., 2002b. Two-group interfacial area transport in vertical air–water flow – ii. Model evaluation. Nuclear Engineering and Design 219 (2), 169–190.

Garnier, C., Lance, M., Marie, J.L., 2002. Measurement of local flow characteristics in buoyancy-driven bubbly flow at high void fraction. Experimental Thermal and Fluid Science 26 (6–7), 811–815.

Grossetete, C., 1995. Caracterisation experimentale et simulations de l'evolution d'un ecoulement diphasique a bulles ascendant dans une conduite verticale, Ph.D. Thesis, Ecole Centrale Paris, France.

Hibiki, T., Hogsett, S., Ishii, M., 1998. Local measurement of interfacial area, interfacial velocity and liquid turbulence in two-phase flow. Nuclear Engineering and Design 184 (2–3), 287–304.

Hibiki, T., Ishii, M., 1999. Experimental study on interfacial area transport in bubbly two-phase flows. International Journal of Heat and Mass Transfer 42 (16), 3019–3035.

Hibiki, T., Ishii, M., 2000a. One-group interfacial area transport of bubbly flows in vertical round tubes. International Journal of Heat and Mass Transfer 43 (15), 2711–2726.

Hibiki, T., Ishii, M., 2000b. Two-group interfacial area transport equations at bubbly-to-slug flow transition. Nuclear Engineering and Design 202 (1), 39–76.

Hibiki, T., Ishii, M., 2002. Distribution parameter and drift velocity of drift-flux model in bubbly flow. International Journal of Heat and Mass Transfer 45 (4), 707–721.

Hibiki, T., Ishii, M., 2003. One-dimensional drift-flux model for two-phase flow in a large diameter pipe. International Journal of Heat and Mass Transfer 46 (10), 1773–1790.

Hibiki, T., Ishii, M., Xiao, Z., 2001. Axial interfacial area transport of vertical bubbly flows. International Journal of Heat and Mass Transfer 44 (10), 1869–1888.

Ishii, M., Chawla, T.C., 1979. Local drag laws in dispersed two-phase flow, Argonne Report Anl-79-105, 52..

Ishii, M., Hibiki, T., 2005. Thermo-fluid Dynamics of Two-phase Flow. Springer, NY.

Ishii, M., Mishima, K., 1984. Two-fluid model and hydrodynamic constitutive relations. Nuclear Engineering and Design 82 (2–3), 107–126.

Ishii, M., Zuber, N., 1979. Drag coefficient and relative velocity in bubbly, droplet or particulate flows. AIChE Journal 25 (5), 843–855.

Kalkach-Navarro, S., 1992. The mathematical modeling of flow regime transition in bubbly two-phase flow, Ph.D. Thesis, Rensselaer Polytechnic Institute, USA.

Khan, A.R., Richardson, J.F., 1987. The resistance to motion of a solid sphere in a fluid. Chemical Engineering Communications 62, 135–150.

Khan, A.R., Richardson, J.F., 1989. Fluid-particle interactions and flow characteristics of fluidized beds and settling suspensions of spherical particles. Chemical Engineering Communications 78, 111–130.

Khan, A.R., Richardson, J.F., 1990. Pressure gradient and friction factor for sedimentation and fluidisation of uniform spheres in liquids. Chemical Engineering Science 45, 255–265.

Kim, S., Sun, X., Ishii, M., Beus, S.G., Lincoln, F., 2002. Interfacial area transport and evaluation of source and sink terms for confined air–water bubbly flow. Nuclear Engineering and Design 219 (1), 61–75.

Kocamustafaogullari, G., Ishii, M., 1995. Foundation of the interfacial area transport equation and its closure relations. International Journal of Heat and Mass Transfer 38 (3), 481–493.

Liu, T.J., 1989. Experimental investigation of turbulence structure in two-phase bubbly flow. Ph.D. Thesis, Northwestern University, USA.

Richardson, J.F., Zaki, W.N., 1954. Sedimentation and fluidization: Part 1. Transactions of the Institution of Chemical Engineers and the Chemical Engineer 32, 35–53.

Serizawa, A., Kataoka, I., Michiyoshi, I., 1991. Phase Distribution in Bubbly Flow. Multiphase Science and Technology. Hemisphere, Washington, DC.

Sun, X., Ishii, M., Kelly, J.M., 2003. Modified two-fluid model for the two-group interfacial area transport equation. Annals of Nuclear Energy 30 (16), 1601–1622.

Sun, X., Kim, S., Ishii, M., Beus, S.G., 2004a. Model evaluation of two-group interfacial area transport equation for confined upward flow. Nuclear Engineering and Design 230, 27–47.

Sun, X., Kim, S., Ishii, M., Beus, S.G., 2004b. Modeling of bubble coalescence and disintegration in confined upward two-phase flow. Nuclear Engineering and Design 230 (1–3), 3–26.

Tomiyama, A., Kataoka, I., Zun, I., Sakaguchi, T., 1998. Drag coefficients of single bubbles under normal and micro gravity conditions. JSME International Journal Series B-Fluids and Thermal Engineering 41, 472–497.

Wallis, G.B., 1974. The terminal speed of single drops or bubbles in an infinite medium. International Journal of Multiphase Flow 1, 491–511.

Wu, Q., Kim, S., Ishii, M., Beus, S.G., 1998. One-group interfacial area transport in vertical bubbly flow. International Journal of Heat and Mass Transfer 41 (8–9), 1103–1112.

Zuber, N., Findlay, J.A., 1965. Average volumetric concentration in two-phase flow systems. Journal of Heat Transfer 87, 453–468.